



저작자표시-비영리-변경금지 2.0 대한민국

이용자는 아래의 조건을 따르는 경우에 한하여 자유롭게

- 이 저작물을 복제, 배포, 전송, 전시, 공연 및 방송할 수 있습니다.

다음과 같은 조건을 따라야 합니다:



저작자표시. 귀하는 원저작자를 표시하여야 합니다.



비영리. 귀하는 이 저작물을 영리 목적으로 이용할 수 없습니다.



변경금지. 귀하는 이 저작물을 개작, 변형 또는 가공할 수 없습니다.

- 귀하는, 이 저작물의 재이용이나 배포의 경우, 이 저작물에 적용된 이용허락조건을 명확하게 나타내어야 합니다.
- 저작권자로부터 별도의 허가를 받으면 이러한 조건들은 적용되지 않습니다.

저작권법에 따른 이용자의 권리는 위의 내용에 의하여 영향을 받지 않습니다.

이것은 [이용허락규약\(Legal Code\)](#)을 이해하기 쉽게 요약한 것입니다.

[Disclaimer](#)

P2X<sub>2</sub> and P2X<sub>4</sub> receptor-mediated  
cation absorption in utricular  
transitional cells and macula

Junhui Jeong

Department of Medicine

The Graduate School, Yonsei University

P2X<sub>2</sub> and P2X<sub>4</sub> receptor-mediated  
cation absorption in utricular  
transitional cells and macula

Directed by Professor Sung Huhn Kim

The Doctoral Dissertation  
submitted to the Department of Medicine,  
the Graduate School of Yonsei University  
in partial fulfillment of the requirements for the degree  
of Doctor of Philosophy

Junhui Jeong

June 2017

This certifies that the Doctoral Dissertation  
of Junhui Jeong is approved.

-----  
Thesis Supervisor : Sung Huhn Kim

-----  
Thesis Committee Member#1 : Jae Young Choi

-----  
Thesis Committee Member#2 : Jinwoong Bok

-----  
Thesis Committee Member#3: Jong Dae Lee

-----  
Thesis Committee Member#4: Wan Namkung

The Graduate School  
Yonsei University

June 2017

## ACKNOWLEDGEMENTS

First and foremost, I would like to thank my supervisor, Professor Sung Huhn Kim for his great supervision and advice to complete this thesis. I also offer my sincerest gratitude to the thesis committee members, Professor Jae Young Choi, Professor Jinwoong Bok, Professor Jong Dae Lee, and Professor Wan Namkung for their constructive advice and encouragement.

In the period of my fellowship in otology, Professor Choi provided general direction to the research of otology. I would like to express my sincere gratitude to him for guiding me to take the first step to research.

In the doctoral course, Professor Kim always encouraged me not to delay but to keep on and accomplish my doctoral dissertation. I would like to give my great thanks to him for offering me an academic insight and passion.

Although I am still insufficient to conduct my own study, I will devote myself to research and continue my efforts based on this dissertation.

Finally, I thank my parents and in-laws, my wife, Jin, and my daughters, Eunjae and Hyojae for supporting and encouraging me to complete this thesis.

I gratefully acknowledge all their help and support once again.

## <TABLE OF CONTENTS>

ABSTRACT .....	1
I. INTRODUCTION .....	3
II. MATERIALS AND METHODS .....	5
1. Trans-epithelial current measurement .....	6
A. Preparation of the utricle .....	6
B. Electrophysiological / pharmacological methods .....	6
C. Solution and chemicals .....	8
D. Data analysis .....	9
2. Immunocytochemistry .....	10
A. Fixation of vestibular labyrinths for cryosections .....	10
B. Immunocytochemistry of the cryosections .....	11
C. Whole-mount fixation and immunocytochemistry .....	12
D. Confocal microscopy .....	13
3. Reverse transcription polymerase chain reaction (RT-PCR) .....	13
III. RESULTS .....	14
1. Cation-absorption in the utricular TCs and macula .....	14
2. Effect of purines and pyrimidines on cation absorption in utricular TCs and macula .....	16
3. ATP-induced cation absorption through non-selective cation channels .....	17
4. Functional evidence of P2X <sub>2</sub> and P2X <sub>4</sub> receptor-mediated cation absorption in utricular TCs and the macula .....	18
5. Cell-specific distribution of P2X <sub>2</sub> and P2X <sub>4</sub> receptors in utricular TCs and the macula .....	22
IV. DISCUSSION .....	25
V. CONCLUSION .....	30
REFERENCES .....	31
ABSTRACT(IN KOREAN) .....	34

## LIST OF FIGURES

Figure 1. A schematic figure of a cross-sectional view of the utricle.....	5
Figure 2. A representative figure of trans-epithelial current measurements from the utricular macula using the scanning vibrating electrode technique. ....	8
Figure 3. Trans-epithelial current changes while a measuring electrode was moved from the dark cell area (roof epithelium) to the utricular macula (10 $\mu$ m/30s). ....	15
Figure 4. Effects of purines and pyrimidines on trans-epithelial currents from transitional cells and the macula. ....	16
Figure 5. Representative figure of the gadolinium effect on ATP-induced cation absorption in transitional cells (A) and macula (B). ....	18
Figure 6. Concentration-response curves for increased current density by ATP analogues in transitional cell (A) and macula (B) areas. ....	20
Figure 7. Inhibitory effect of P2X receptor blockers on ATP-induced current density in the transitional cell area. ·	20
Figure 8. Inhibitory effect of P2X receptor blockers on ATP-induced current density in the macula. ....	21
Figure 9. Immunocytochemistry of P2X <sub>2</sub> in the vestibular	

labyrinth. ....	23
Figure 10. P2X <sub>4</sub> receptor mRNA expression in the utricle (RT-PCR). ....	24

## LIST OF TABLES

Table 1. Primers used for reverse transcription polymerase chain reaction (RT-PCR) ....	14
--	----



## ABSTRACT

P2X<sub>2</sub> and P2X<sub>4</sub> receptor-mediated cation absorption in utricular transitional cells and macula

Junhui Jeong

*Department of Medicine  
The Graduate School, Yonsei University*

(Directed by Professor Sung Huhn Kim)

Adenosine 5'-triphosphate (ATP) regulates inner ear function by modulating ion transport through purinergic receptors in inner ear epithelial cells. This study was designed to investigate purinergic receptor-mediated cation transport by mouse utricular macula and the surrounding transitional cells (TCs), where linear acceleration stimuli are sensed. Among ATP, adenosine 5'-diphosphate (ADP), uridine 5'-triphosphate (UTP), and uridine 5'-diphosphate (UDP), only ATP (100  $\mu$ M) induced cation absorption currents in TCs and macula. The current was almost completely inhibited by the application of gadolinium (100  $\mu$ M). The order of agonist potencies for the cation absorption current was ATP > 3'-O-(4-benzoyl-benzoyl) adenosine 5'-triphosphate (bzATP) >>  $\alpha,\beta$ -methyleneadenosine 5' -triphosphate ( $\alpha\beta$ meATP) in both TCs and macula, and the EC<sub>50</sub> (concentration that produces a half-maximal effect) values for ATP, bzATP, and  $\alpha\beta$ meATP were 27.2  $\mu$ M, 43.9  $\mu$ M, and 34.5  $\mu$ M in the TCs and 20.7  $\mu$ M, 63.4  $\mu$ M, and 2014.1  $\mu$ M in the macula, respectively (EC<sub>50</sub> values of  $\alpha\beta$ meATP were not definitively identified due to the low potency of  $\alpha\beta$ meATP). The ATP-induced current was partially blocked by suramin (100  $\mu$ M), pyridoxal phosphate-6-azo(benzene-2,4-disulfonic acid) (PPADS) (10  $\mu$ M), and 5-(3-bromophenyl)-1,3-dihydro-2H-benzofuro[3,2-e]-1,4

-diazepin-2-one (5-BDBD) (5  $\mu$ M) and was almost completely blocked by PPADS + 5-BDBD in both areas. Immunocytochemistry revealed that P2X<sub>2</sub> receptors were distributed in TCs and supporting cells in the macula; however, only P2X<sub>4</sub> receptor was not detected in the macula by immunocytochemistry, but only its mRNA expression was detected there. These results indicate that ATP induces cation absorption through P2X<sub>2</sub> and P2X<sub>4</sub> receptors in utricular TCs and the macula. P2X<sub>2</sub> and P2X<sub>4</sub>-mediated cation transport likely provides a cation shunt under conditions of excessive linear acceleration, thereby protecting hair cells by reducing their cation burden.

---

Key words : utricle, transitional cell, macula, receptor, cation

P2X<sub>2</sub> and P2X<sub>4</sub> receptor-mediated cation absorption in utricular  
transitional cells and macula

Junhui Jeong

*Department of Medicine  
The Graduate School, Yonsei University*

(Directed by Professor Sung Huhn Kim)

I. INTRODUCTION

The utricle is a part of the vestibular organs of the inner ear and is involved in maintaining balance by detecting linear acceleration. The sensory epithelium of the utricle is called the macula, which is composed of the otolithic membrane, hair cells (HCs), and supporting cells (SCs), and the macula transits into transitional cells (TCs) in the periphery (Figure 1.). Linear acceleration of the head induces movement of the otolithic membrane, which causes the displacement of HC stereocilia. Displacement in the direction of the kinocilium, which is the longest stereocilium, modulates the opening of mechano-sensitive non-selective cation channels at the stereocilia, which induces K<sup>+</sup> influx into HCs. This series of movements results in the depolarization of HCs, which causes Ca<sup>2+</sup> influx through voltage-gated Ca<sup>2+</sup> channels and finally causes neurotransmitter release at the basolateral surface of HCs to propagate electrical signals to the central nervous system through vestibular nerve fibers.<sup>1</sup> The

generation of electrical signals in HCs to maintain normal balance requires a luminal fluid with a distinct ionic composition (high  $[K^+]$  and low  $[Na^+]$ ), known as the endolymph. The unique ion composition of the endolymph is maintained by the activity of various ion channels in the inner ear epithelial cells and their regulatory materials in the fluid.<sup>2</sup> Adenosine 5'-triphosphate (ATP) is one of the paracrine materials secreted into the endolymphatic space in response to mechanical stimulation to the inner ear, such as by loud noise, and is involved in regulating inner ear ion concentrations through purinergic receptors on the inner ear epithelium.<sup>3</sup> Purinergic receptors are thought to play a role in protecting the inner ear from severe mechanical stress induced by loud noise or excessive acceleration by regulating endolymphatic cation concentrations.<sup>3,4</sup> ATP-stimulated cation absorption through purinergic receptors by inner ear epithelial cells, such as cochlear outer sulcus cells and vestibular ampullary TCs, reduces the  $K^+$  burden on sensory HCs.<sup>5</sup> The utricular macula can exhibit similar purinergic receptor-mediated ion transport, in that both the vestibular ampulla and the utricle have similar cell types, although the role of each organ is different (detection of angular acceleration and linear acceleration for the ampulla and the utricle, respectively). Additionally, purinergic signaling-mediated cation transport is likely to occur more vigorously in the utricle because the surface area of TCs and the sensory epithelium is larger than that of the ampulla. However, nothing has been revealed regarding purinergic receptor-mediated ion transport and receptor types / subunits in the utricular TC.

Moreover, the role of purinergic receptors in the macular region remains unclear.

In this study, we investigated purinergic receptor-mediated ion transport in the utricular TC and macular area using electrophysiological, pharmacological, and molecular biological methods. This study will elucidate the mechanisms of endolymphatic ion concentration regulation as a mechanism by which vestibular organs protect themselves from excessive mechanical stress.

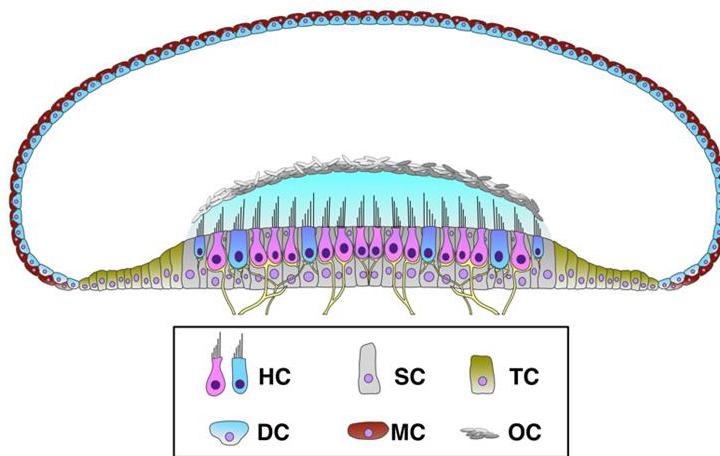


Figure 1. A schematic figure of a cross-sectional view of the utricle. Hair cells (HCs), supporting cells (SCs), and the otolithic membrane, a thin layer of otoconia (OC), comprise the utricular macula. Transitional cells (TCs) are located in the periphery of the macula. The utricular roof epithelium was composed of dark cells (DCs) and melanocytes (MCs).

## II. MATERIALS AND METHODS

## 1. Trans-epithelial current measurement

### A. Preparation of the utricle

C57BL/6 mice (6-8 weeks old) were anesthetized by i.p. injection with 30 mg/kg tiletamine-zolazepam (Zoletil<sup>®</sup>; Virbac, Carros, France) and 10 mg/kg xylazine (Rompun<sup>®</sup>; Bayer, Leverkusen, Germany) and were sacrificed by decapitation. Temporal bones were dissected, and the complete membranous labyrinth of the vestibule was carefully removed from the temporal bone in perilymph-like physiologic saline (see C. Solution and chemicals). Then, the utricle was excised from the labyrinth, and the utricular roof epithelium was carefully removed. After removal of the roof epithelium, the otolithic membrane was carefully removed from the utricular macula, and the macula was folded with the luminal side facing outward, similar to a previously reported method.<sup>6</sup> The tissue was mounted in a perfusion chamber on an inverted microscope (IX51<sup>®</sup>; Olympus, Tokyo, Japan) and continuously perfused with perilymph-like physiologic saline at an exchange ratio of 1.1 times/s.

### B. Electrophysiological / pharmacological methods

The scanning vibrating electrode technique (SVET) was used to measure the current in the TC and macular areas under short circuit conditions, as reported previously.<sup>6</sup> Each area of the utricular macula was distinguishable via microscopy ( $\times 100$ ), and the trans-epithelial current from each cell area was measured by positioning the probe at each area (Figure 2. and 3.). To avoid

interference from the trans-epithelial current from each area, the probe was positioned as far as possible ( $> 30 \mu\text{m}$ ) from the utricular macula when measuring the current from the TC area, and vice versa. Because the spatial resolution of the SVET system is reported to be  $10\text{-}30 \mu\text{m}$ ,<sup>7,8</sup> the current interference at these positions was minimal. Current density was monitored using a vibrating platinum-iridium wire microelectrode that was insulated with parlene-C (Micro Electrodes, Gaithersburg, MD, USA) and coated with platinum black on the exposed tip. The electrode tip of the probe was vibrated at two frequencies between 400 and 700 Hz along a horizontal ( $x$ ) and vertical ( $z$ ) axis by piezo-electric bimorph elements (Applicable Electronics, Forestdale, MA, USA) and was positioned  $10 \pm 2 \mu\text{m}$  from the apical surface of the epithelium. The  $x$ -axis was perpendicular to the face of the epithelium. A platinum-black electrode served as a reference in the bath chamber. The signals from the oscillators driving the probe, which were connected to a dual-channel phase-sensitive detector (Applicable Electronics, Forestdale, MA, USA), were digitized (16 bit) at a rate of 0.5 Hz. The electrode was positioned where the current density showed a maximum  $x$  value and minimum  $z$  value. Data derived from the  $x$  direction current density were plotted with Origin software, version 8.0. (OriginLab Software, Northampton, MA, USA).

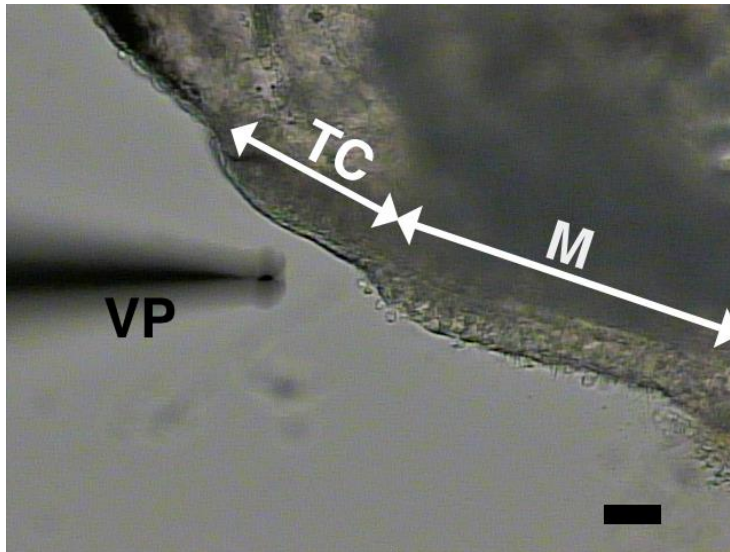


Figure 2. A representative figure of trans-epithelial current measurements from the utricular macula using the scanning vibrating electrode technique. The trans-epithelial current under short circuit conditions was measured in the transitional cell (TC) area or mucular (M) area, which was easily identified by the presence of stereocilia. VP: vibrating probe. Scale bar: 50  $\mu$ m.

### C. Solution and chemicals

For electrophysiological experiments, a perilymph-like physiological saline solution [150 mM NaCl, 3.6 mM KCl, 1 mM MgCl<sub>2</sub>, 0.7 mM CaCl<sub>2</sub>, 5 mM glucose, and 10 mM 4-(2-hydroxyethyl)-1-piperazineethanesulfonic acid (HEPES) (pH 7.4)] was used for perfusion. ATP (A9187; Sigma, St. Louis, MO, USA),  $\alpha,\beta$ -methyleneadenosine 5'-triphosphate ( $\alpha\beta$ meATP) (M6517; Sigma, St. Louis, MO, USA), 3'-O-(4-benzoyl-benzoyl)adenosine 5'-triphosphate



(BzATP) (B6396; Sigma, St. Louis, MO, USA), uridine 5'-triphosphate (UTP) (U6875; Sigma, St. Louis, MO, USA), pyridoxal phosphate-6-azo(benzene-2,4-disulfonic acid) (PPADS) (P178; Sigma, St. Louis, MO, USA), suramin (S2671; Sigma, St. Louis, MO, USA), and gadolinium chloride ( $GdCl_3$ ) (G7532; Sigma, St. Louis, MO, USA) were directly dissolved in perilymph-like physiological saline just before use. Adenosine 5'-diphosphate (ADP) (A2754; Sigma, St. Louis, MO, USA) and uridine 5'-diphosphate (UDP) (U4125; Sigma, St. Louis, MO, USA) were pre-incubated for 1.5-2 hr at room temperature with hexokinase (1 U/ml) (H4502; Sigma, St. Louis, MO, USA) and glucose (5 mM) to eliminate the possibility of minor ATP and UTP contamination. All purinergic agonists were applied to the bath briefly (7-10 sec) to avoid receptor desensitization and applied once more after the application of all chemicals to confirm receptor activity. Bumetanide (10  $\mu$ M) (B3023; Sigma, St. Louis, MO, USA), a  $Na^+K^+2Cl^-$  cotransporter inhibitor, was continuously perfused during the experiment in the TC area to prevent any possible current density interference by the  $K^+$  secretion current from the adjacent dark cell area.

#### D. Data analysis

Results are presented as the mean  $\pm$  standard error from n observations. Purine and pyrimidine-induced current was calculated by subtracting the baseline current from the peak point of the purine and pyrimidine-induced current. Baseline current was calculated by averaging the current density from 1 to 1.25

min, when the probe was located at the apical side of each TC and HC area. The significance of the current changes between the two points (baseline and peak point of the induced-current) was calculated using Student's t-test. The effects of purinergic receptor blockers were calculated by subtracting the peak value after ATP application during the perfusion of purinergic receptor blockers from the peak point after ATP application without the application of purinergic receptor blockers. The differences in the effects of the purinergic receptor blockers were calculated using one-way analysis of variance (ANOVA) with Holm-Sidak's post-test.  $p < 0.05$  was considered significant. The concentration dependence of the purine agonists was analyzed using the Hill equation;  $I = I_{\max} [C^h / (EC_{50} + C^h)]$ , where  $I_{\max}$  is current in the presence of saturating concentrations of the agonist,  $C$  is the concentration of the agonist,  $h$  is the Hill coefficient, and  $EC_{50}$  is the concentration that produces a half-maximal effect.

## 2. Immunocytochemistry

### A. Fixation of vestibular labyrinths for cryosections

Deeply anesthetized mice were sacrificed by decapitation. The vestibular labyrinth was isolated by microdissection in Cl<sup>-</sup>-free solution and transferred to fixative. The Cl<sup>-</sup>-free solution contained 150 mM Na-gluconate, 1.6 mM K<sub>2</sub>HPO<sub>4</sub>, 0.4 mM KH<sub>2</sub>PO<sub>4</sub>, 4 mM Ca-gluconate<sub>2</sub>, 1 mM MgSO<sub>4</sub> and 5 mM glucose, pH 7.4. The fixative consisted of 4% formaldehyde (Electron Microscopy Sciences, Hatfield, PA, USA) in phosphate buffered saline (PBS),

which contained 137 mM NaCl, 10.1 mM Na<sub>2</sub>HPO<sub>4</sub>, 1.8 mM KH<sub>2</sub>PO<sub>4</sub>, and 2.7 mM KCl, pH 7.4. The isolated vestibular labyrinths were fixed for 1-2 hr at room temperature.

#### B. Immunocytochemistry of the cryosections

Fixed tissues were processed through a sucrose gradient, infiltrated with polyethylene glycol, and then sectioned (6 μm) (CM3050S<sup>®</sup>; Leica, Nussloch, Germany). The cryosections were blocked with 5% BSA in PBS-TX (PBS with 0.15% Triton X-100 and 5% bovine serum albumin). The slides were incubated overnight at 4°C with primary antibody in 2.5% BSA PBS-TX. The following primary antibodies were used: unconjugated rabbit anti-P2X<sub>2</sub> (1:200, APR-003; Alomone Labs, Jerusalem, Israel) and Atto-594 conjugated rabbit anti-P2X<sub>2</sub> (1:200, APR-003-AR; Alomone Labs, Jerusalem, Israel), which were raised against (C)SQQDSTSTDPKGLAQL (amino acids 470-485 of the mouse P2X<sub>2</sub> receptor, GenBank: Q8K3P1), unconjugated rabbit anti-P2X<sub>4</sub> (1:200, APR-002; Alomone Labs, Jerusalem, Israel) that was raised against the intracellular epitope (C)KKYKYVEDYEQGLSGEMNQ (amino acids 348-366 of the mouse P2X<sub>4</sub> receptor, GenBank: Q9JJX6.1), unconjugated rabbit anti-P2X<sub>4</sub> (1:200, APR-024; Alomone Labs, Jerusalem, Israel) that was raised against the extracellular epitope (C)RDLAGKEQRTLTK (amino acids 301-313 of the mouse P2X<sub>4</sub> receptor, GenBank: Q9JJX6.1), and unconjugated goat anti-P2X<sub>4</sub> (1:100, ab134559; Abcam, Cambridge, MA, USA) that was raised against

(C)ETDSVVSSVTTKAK (amino acids 56-69 of the mouse P2X<sub>4</sub> receptor, GenBank: Q9JJX6.1). Slides were washed with PBS-TX and incubated for 1 h at room temperature with phalloidin 488 (1:40; Invitrogen, Carlsbad, CA, USA), 4',6-diamidino-2-phenylindole (DAPI) (1:1,000; Invitrogen, Carlsbad, CA, USA), and, if appropriate, secondary antibody (1:1,000, goat anti-rabbit Alexa 594; Invitrogen, Carlsbad, CA, USA). After staining, the slides were washed and cover-slipped with mounting medium (FluorSave, Cat#: 345789; EMD-Millipore, Darmstadt, Germany).

### C. Whole-mount fixation and immunocytochemistry

Vestibular labyrinths were isolated by microdissection in Cl<sup>-</sup>-free solution. Utricular maculae were isolated, and otolithic membranes were manually removed using fine glass needles. Isolated utricular maculae that were free of otoconia material were fixed for 1-2 hr at room temperature. The fixed tissues were washed in PBS-TX, blocked for 1 h with 5% BSA in PBS-TX, and incubated overnight at 4°C with primary antibodies in 2.5% BSA PBS-TX. The tissues were washed with PBS-TX and incubated for 1 hr at room temperature with phalloidin 488 (1:40), DAPI (1:1,000), and where appropriate, with secondary antibody (1:1,000, goat anti-rabbit Alexa 594). After staining, the utricular maculae were washed and cover-slipped with mounting medium (FluorSave) on slides that were prepared with nail-polish to act as a spacer to avoid squeezing of the tissue.

#### D. Confocal microscopy

Immunocytochemistry of cryosections and whole mounts was viewed by confocal microscopy (LSM 880<sup>®</sup>; Carl Zeiss, Jena, Germany).

#### 3. Reverse transcription polymerase chain reaction (RT-PCR)

P2X<sub>4</sub> receptor transcripts were detected using RT-PCR. Utricles were carefully dissected from the mouse temporal bone, and the roof epithelium was carefully removed as described above. After homogenization of the harvested utricles, total ribonucleic acid (RNA) was extracted using TRIzol<sup>®</sup> (Invitrogen, Carlsbad, CA, USA) following the manufacturer's protocol. The quantity and quality of the isolated RNA were determined using a NanoDrop ND-100 spectrophotometer (NanoDrop Technologies, Wilmington, DE, USA) and by analyzing the 18S and 28S ribosomal RNA (rRNA) bands after electrophoresis. Complementary deoxyribonucleic acid (cDNA) was synthesized from 3 µg of total RNA using random hexamer primers (Perkin Elmer Life Sciences, Boston, MA, USA; and Roche Applied Science, Mannheim, Germany), Avian myeloblastosis virus (AMV) reverse transcriptase (Perkin Elmer Life Sciences, Boston, MA, USA), and ribonuclease (RNase) inhibitor (Perkin Elmer Life Sciences, Boston, MA, USA). Reverse transcription was performed for 10 min at room temperature, 30 min at 50°C, and 15 min at 95°C. The P2X<sub>4</sub> receptor messenger RNA (mRNA) was amplified using gene-specific primers (Table 1).

The PCR conditions included 30 cycles of denaturation at 94°C for 30 s, annealing at 59°C for 30 s, and polymerization at 72°C for 30 s. The PCR products were run on a 1.5% agarose gel and visualized with ethidium bromide under a transilluminator. The PCR products were purified with a PCR purification kit (Qiagen, Valencia, CA, USA) and the purified PCR products were sequenced to verify the identity of the RT-PCR product.

Table 1. Primers used for reverse transcription polymerase chain reaction (RT-PCR)

Gene	GenBank accession number		Primer (5' → 3')	Amplicon size (base pair)
18S RNA	BK000964	Forward	GAGGTTCGAAGACGATCAGA	315
		Reverse	TCGCTCCACCAACTAAGAAC	
P2X <sub>4</sub>	NM_001310720	Forward	AGTGGGACTGCAACCTTGAC	219
		Reverse	CAAACCTTGCCAGCCTTTCCAA	
		Forward	AAGTGGGACTGCAACCTTGA	222
		Reverse	GTCAAACCTTGCCAGCCTTTCC	

RNA: ribonucleic acid.

### III. RESULTS

#### 1. Cation absorption in the utricular TCs and macula

$K^+$  secretion currents were detected when the probe was moved close to the dark cell area of the roof epithelium, and the current decreased as the probe was moved from the dark cell area to the TC area (Figure 3.). The current vector changed to cation absorption when the probe was located in the TC area, and the cation absorption current continued until the probe was moved to the macula (Figure 3.). The mean density of the current was  $-6.4 \pm 1.0 \mu A/cm^2$  in the TC area (n=34) and  $-6.9 \pm 1.0 \mu A/cm^2$  in the macula (n=47).

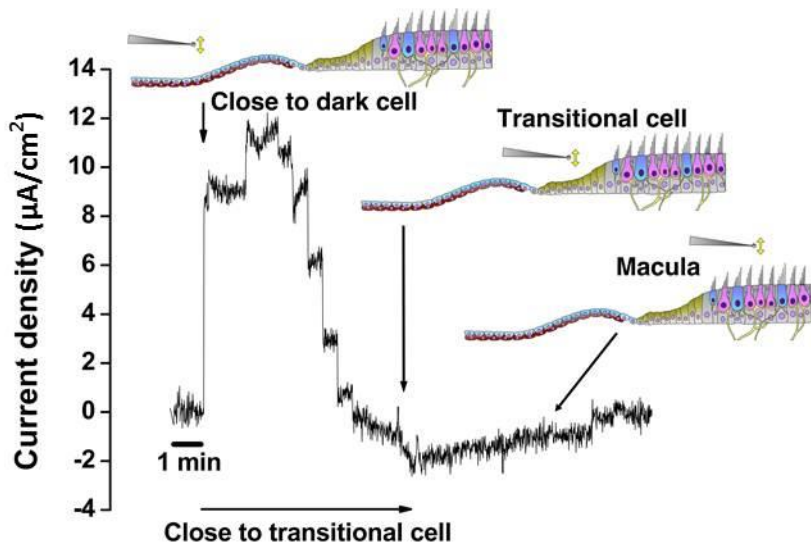


Figure 3. Trans-epithelial current changes while a measuring electrode was moved from the dark cell area (roof epithelium) to the utricular macula ( $10\mu m/30s$ ). Cation secretion current from the dark cell area changed into cation absorption current in the transitional cell and macular areas.

## 2. Effect of purines and pyrimidines on cation absorption in utricular TCs and macula

When purines and pyrimidine such as ATP (100  $\mu$ M), ADP (100  $\mu$ M), UTP (100  $\mu$ M), and UDP (100  $\mu$ M) were perfused, the cation absorption currents were only significantly induced after ATP application in both the TC area and the macula [amount of current change:  $-161.7 \pm 50.6 \mu\text{A}/\text{cm}^2$  in the TC area ( $n=5$ ) and  $-65.2 \pm 22.1 \mu\text{A}/\text{cm}^2$  in the macula ( $n=5$ ),  $p<0.001$ , Figure 4.]. The effects of the other agonists, which mainly act on mouse P2Y receptors, on current density were insignificant ( $p>0.05$ , Figure 4.). This result implies that ATP modulated cation absorption mainly through P2X receptors.

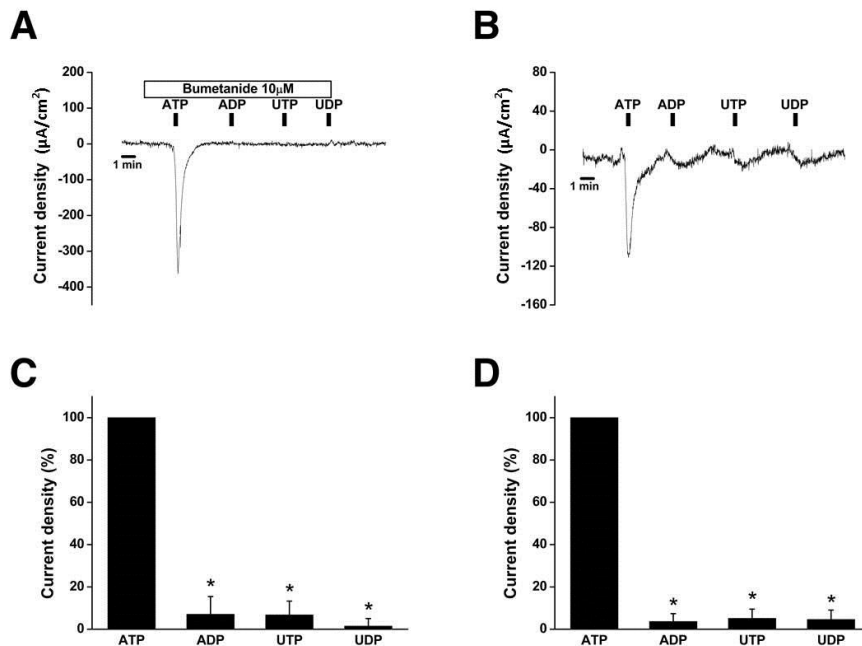


Figure 4. Effects of purines and pyrimidines on trans-epithelial currents from



transitional cells and the macula. A, B. Representative figures of the current change after the application of purines and pyrimidines in transitional cells and the macula, respectively. C, D. Summary of the current density change ratios after purine and pyrimidine application on transitional cells and the macula, respectively (n=5 for each experiment). \* $p<0.05$ . ATP: Adenosine 5'-triphosphate, ADP: Adenosine 5'-diphosphate, UTP: uridine 5'-triphosphate, UDP: uridine 5'-diphosphate.

### 3. ATP-induced cation absorption through non-selective cation channels

We investigated if ATP-induced cation absorption occurred through non-selective cation channels formed by P2X receptors, as shown previously in ampullary TCs.<sup>5</sup> Application of Gd (100  $\mu$ M) significantly decreased the ATP-induced cation absorption current in both the TC and macula areas [ATP-induced current decreased to  $21.2 \pm 5.3\%$  and  $21.4 \pm 9.4\%$  of that in the TC area (n=6) and macula (n=5), respectively.  $p<0.001$ , Figure 5.]. This result indicates that ATP increased cation-absorption mainly through non-selective cation channels (e.g., P2X receptors) in TCs and in other epithelial cells in the macula.

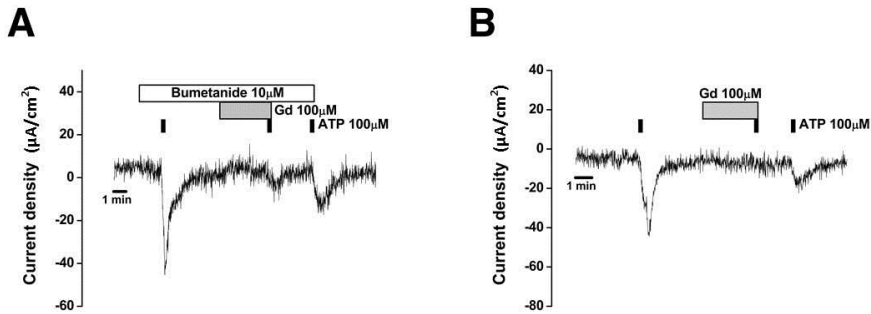


Figure 5. Representative figure of the gadolinium effect on ATP-induced cation absorption in transitional cells (A) and macula (B). Gd: gadolinium, ATP: Adenosine 5'-triphosphate.

#### 4. Functional evidence of P2X<sub>2</sub> and P2X<sub>4</sub> receptor-mediated cation absorption in utricular TCs and the macula

To investigate P2X receptor subunits in utricular TCs and in other epithelial cells in the macula, agonist potencies using ATP analogues, such as ATP, bzATP, and  $\alpha\beta\text{meATP}$ , were compared. Dose-response experiments revealed that the order of agonist potencies for cation absorption current was  $\text{ATP} > \text{bzATP} \gg \alpha\beta\text{meATP}$  in both the TC area and macula (Figure 6.). The  $\text{EC}_{50}$  values calculated from the Hill equation for ATP, bzATP, and  $\alpha\beta\text{meATP}$  were 27.2  $\mu\text{M}$ , 43.9  $\mu\text{M}$ , and 34.5  $\mu\text{M}$  (not definitively identified due to the low potency of  $\alpha\beta\text{meATP}$ ) in the TC area and 20.7  $\mu\text{M}$ , 63.4  $\mu\text{M}$ , and 2014.1  $\mu\text{M}$  (not definitively identified due to the low potency of  $\alpha\beta\text{meATP}$ ) in the macula ( $n=4$  for each experiment), respectively. The order of the agonist potencies and  $\text{EC}_{50}$

values were consistent with the reported characteristics of P2X<sub>2</sub> and P2X<sub>4</sub> receptors (reported EC<sub>50</sub> values of ATP, bzATP, and  $\alpha\beta$ meATP are 2-8, 6-30, and >100  $\mu$ M for P2X<sub>2</sub> and 1-10, 3, and 4-300  $\mu$ M for P2X<sub>4</sub> receptor).<sup>9</sup>

Then, we applied P2X receptor blockers to investigate which subunit mediated ATP-induced cation absorption. We first used suramin (100  $\mu$ M) and PPADS (10  $\mu$ M) because these concentrations have been shown to completely block P2X<sub>2</sub> receptor function while minimally affecting P2X<sub>4</sub> receptor activity.<sup>9</sup> The application of suramin and PPADS partially decreased ATP-induced cation absorption both in the TC area and the macula [suramin decreased the ATP-induced current to  $47.0 \pm 8.8\%$  and  $33.1 \pm 4.6\%$  of that in the TC area (n=5) and macula (n=5), respectively; PPADS decreased the ATP-induced current to  $46.1 \pm 4.4\%$  and  $41.8 \pm 3.8\%$  of that in the TC area (n=5) and macula (n=5), respectively;  $p < 0.05$ , Figure 7A, B, and E.; Figure 8A, B, and E.]. ATP-induced cation absorption current was also partially decreased both in the TC area and macula when 5-(3-bromophenyl)-1,3-dihydro-2H-benzofuro [3,2-e]-1,4-diazepin-2-one (5-BDBD) (5  $\mu$ M), a specific P2X<sub>4</sub> receptor blocker, was applied [ATP-induced current decreased to  $46.8 \pm 5.8\%$  and  $41.6 \pm 8.8\%$  of that in the TC area (n=5) and macula (n=5), respectively,  $p < 0.05$ , Figure 7C and E.; Figure 8C and E.]. Combined application of PPADS and 5-BDBD almost completely inhibited ATP-induced cation absorption in both the TC area and macula [current decreased to  $6.0 \pm 4.9\%$  and  $9.9 \pm 7.8\%$  of that in the TC area (n=5) and macula (n=5), respectively,  $p < 0.05$ , Figure 7D and E.; Figure 8D and

E.]. These results imply that both the P2X<sub>2</sub> and P2X<sub>4</sub> receptors modulated ATP-induced cation absorption in TCs and the macula.

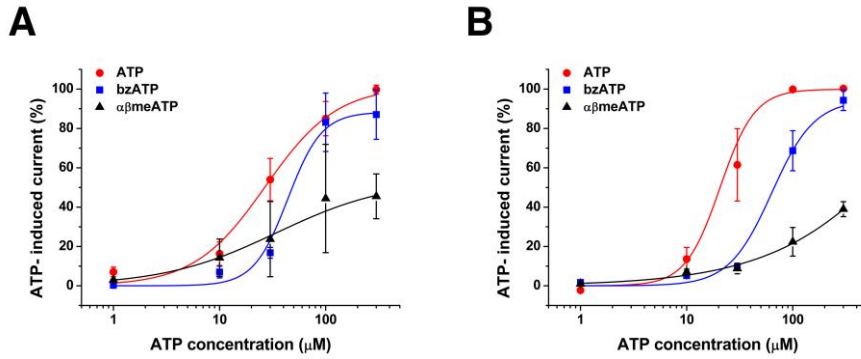


Figure 6. Concentration-response curves for increased current density by ATP analogues in transitional cell (A) and macula (B) areas. Curves are best fits to the Hill equation ( $n=4$  for each experiment). ATP: Adenosine 5'-triphosphate, bzATP: 3'-O-(4-benzoyl-benzoyl) adenosine 5'-triphosphate,  $\alpha\beta$ meATP:  $\alpha,\beta$ -methyleneadenosine 5'-triphosphate.

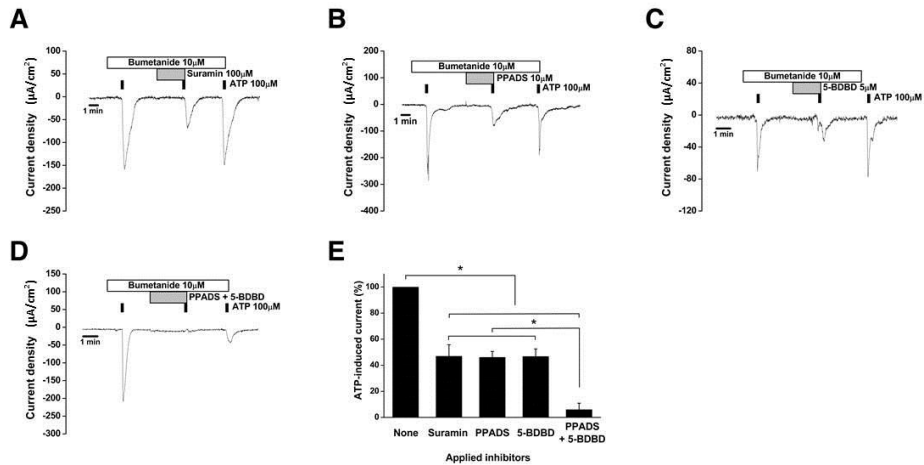


Figure 7. Inhibitory effect of P2X receptor blockers on ATP-induced current

density in the transitional cell area. A-D. Representative figures for the effects of suramin (100  $\mu$ M), PPADS (10  $\mu$ M), 5-BDBD (5  $\mu$ M), and PPADS + 5-BDBD on ATP- induced current density. E. Summary of the inhibitory effects of the blockers on ATP-induced current density (n=5). \*  $p$ <0.05. ATP: Adenosine 5'-triphosphate, PPADS: pyridoxal phosphate-6-azo(benzene- 2,4-disulfonic acid), 5-BDBD: 5-(3-bromophenyl)-1,3-dihydro-2H-benzofuro [3,2-e]-1,4-diazepin-2-one.

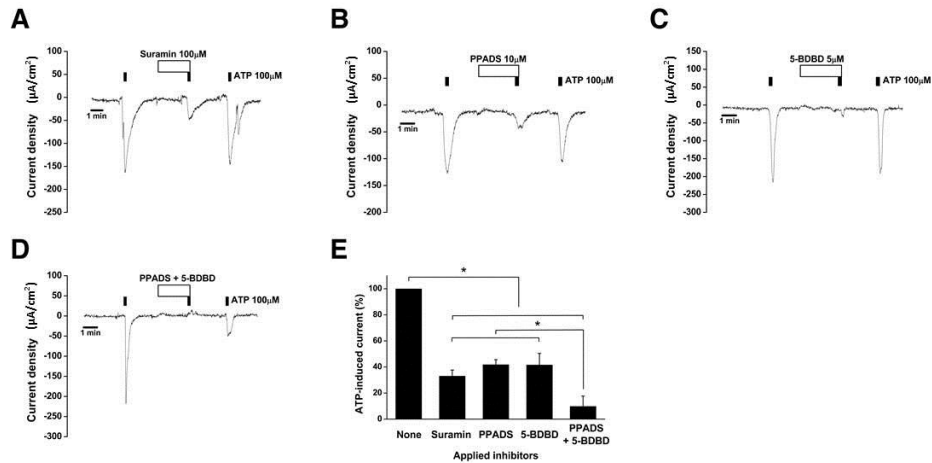


Figure 8. Inhibitory effect of P2X receptor blockers on ATP-induced current density in the macula. A-D. Representative figures for the effects of suramin (100  $\mu$ M), PPADS (10  $\mu$ M), 5-BDBD (5  $\mu$ M), and PPADS + 5-BDBD on ATP-induced current density. E. Summary of the inhibitory effects of the blockers on ATP-induced current density (n=5). \*  $p$ <0.05. ATP: Adenosine 5'-triphosphate, PPADS: pyridoxal phosphate-6-azo(benzene- 2,4-disulfonic

acid), 5-BDBD: 5-(3-bromophenyl)-1,3-dihydro-2H-benzofuro [3,2-e]-1,4-diazepin-2-one.

#### 5. Cell-specific distribution of P2X<sub>2</sub> and P2X<sub>4</sub> receptors in utricular TCs and the macula

Consistent with previous results,<sup>5</sup> P2X<sub>2</sub> receptors were identified in TCs of the vestibular ampulla (Figure 9A and C.). In the utricle, receptor expression was detected in TCs and SCs in the macula, but not in HCs in the macula (Figure 9B, D-J.). This finding suggested that the ATP-induced cation absorption current is mediated by P2X<sub>2</sub> receptors in utricular TCs and SCs. For P2X<sub>4</sub> receptors, despite using several antibodies, we were unable to identify specific P2X<sub>4</sub> receptor expression in the ampulla and utricle. However, further examination using RT-PCR revealed the presence of P2X<sub>4</sub> mRNA expression in the utricle (Figure 10.), although we were unable to identify the definite location of P2X<sub>4</sub> receptors in the utricle. Therefore, whether the P2X<sub>4</sub>-mediated current originated from SCs or HCs in the macula remains unclear, although the current clearly originated from TCs, because no other cell types are present in the TC area in utricle.

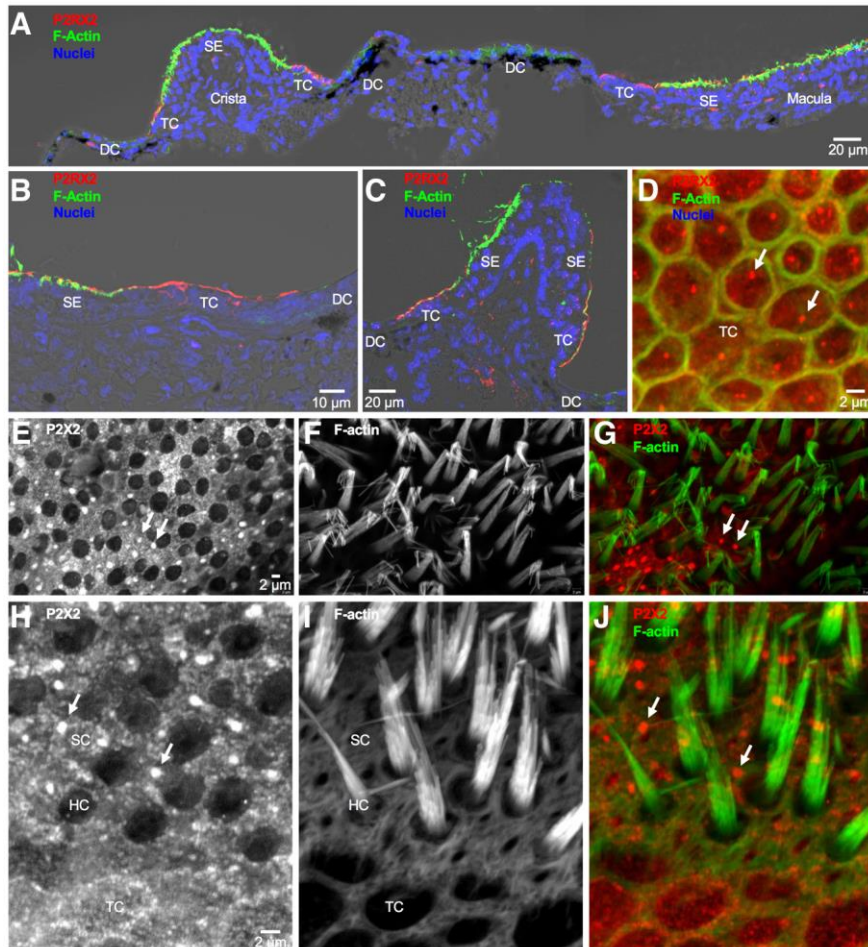


Figure 9. Immunocytochemistry of P2X<sub>2</sub> in the vestibular labyrinth. Data shown were obtained using a fluorescent-dye conjugated anti-P2X<sub>2</sub> antibody. Similar observations were made using an unconjugated anti-P2X<sub>2</sub> antibody. A-C. Cryosections of the utricular macula and the crista of the anterior semicircular canal. P2X<sub>2</sub> (red) expression was detected in the apical membrane of transitional cells (TCs) and in the apical membranes of cells in the sensory epithelium (SE). Transitional cells are situated between the sensory epithelium

and vestibular dark cells (DC). The sensory epithelium was marked by heavy filamentous actin (F-actin) staining (green). Vestibular dark cells were identified as epithelial cells overlaying pigmented cells in the underlying connective tissue. D. A whole-mount of the utricular macula. P2X<sub>2</sub> expression (red) was observed throughout the apical membranes of TCs. In many cells, P2X<sub>2</sub> expression was concentrated in hot spots (arrows). Individual TCs were outlined with F-actin expression (green) near tight junctions. E-J. Whole-mounts of the utricular macula. P2X<sub>2</sub> expression (white or red) in the sensory epithelium was found in the apical membranes of supporting cells (SCs) and TCs but not in sensory hair cells (HCs). Sensory HCs were identified by F-actin staining (white or green) of hair bundles. P2X<sub>2</sub> expression in the apical membranes of many SCs appeared to be concentrated in hot spots (arrows).

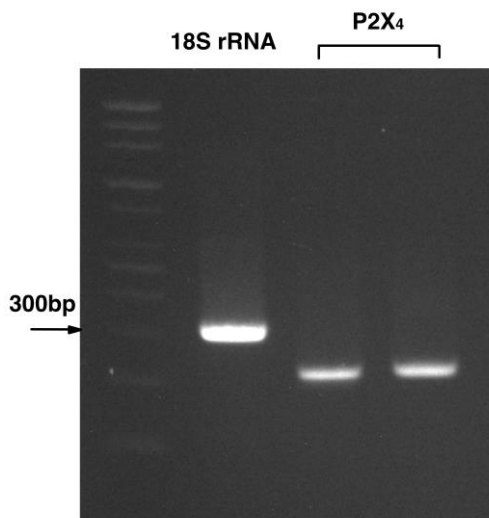




Figure 10. P2X<sub>4</sub> receptor mRNA expression in the utricle (RT-PCR). Transcripts were detected using two different primers for P2X<sub>4</sub> receptor. mRNA: messenger ribonucleic acid, rRNA: ribosomal ribonucleic acid, bp: base pair.

#### IV. DISCUSSION

ATP is reportedly secreted in response to excessive noise stimulation in the cochlea, where sound stimulation is transformed into electrical signals to propagate the transduction of the stimulus to the central nervous system.<sup>10</sup> The main sites for ATP secretion were suggested to be strial marginal cells, supporting cells, and the organ of Corti,<sup>11,12</sup> and secreted ATP modulates signal transduction by HCs via P2X<sub>2</sub> and P2Y<sub>2</sub> receptors by regulating cation (mainly K<sup>+</sup>) secretion and absorption in hair cells and neighboring epithelial cells.<sup>3,12</sup> Similarly, the modulation of cation secretion and absorption by ATP via P2X<sub>2</sub> and P2Y<sub>2</sub> receptors was observed in the vestibular system of gerbils through functional studies. ATP induces cation absorption in ampullary TCs via P2X<sub>2</sub> receptors and inhibits cation secretion in utricular dark cells via P2Y<sub>2</sub> receptors, which ultimately reduces the cation burden on vestibular HCs.<sup>5</sup> Although ATP secretion in the vestibular system has not been definitively identified, ATP is expected to be secreted by vestibular dark cells and supporting cells because of the structural and functional similarity between strial marginal cells/cochlear supporting cells and vestibular dark cells/vestibular supporting cells.<sup>13</sup> ATP is likely to be involved in the modulation of cation transport in vestibular epithelial cells following excessive mechanical stimulation, such as abrupt

acceleration, as occurs in cochlear epithelial cells. Although purinergic receptor-mediated cation transport was reported in ampullary TCs and utricular dark cells,<sup>3</sup> there are more studies about purinergic receptor-mediated ion transport in the cochlea than in the vestibular system. However, the vestibular organ is the primary site for managing balance maintenance; thus, the role of these receptors in this system should be very important because the dysfunction of these receptors can cause balance disorders, even in response to ordinary acceleration that occurs in daily life.

In the present study, we identified ATP-induced cation absorption in the TCs and macula of the mouse utricle. A unique finding of this study is the co-involvement of P2X<sub>4</sub> receptors in addition to P2X<sub>2</sub> receptors in ATP-induced cation absorption in utricular TCs, which differs from the finding in ampullary TCs, where only P2X<sub>2</sub> receptor involvement in current was identified. Furthermore, this study is the first to functionally identify ATP-induced cation absorption mediated by P2X<sub>2</sub> and P2X<sub>4</sub> receptors in the utricular macula. P2X<sub>2</sub> receptors were distributed in macular supporting cells, although the specific cell types in the macular where the P2X<sub>4</sub> receptors were distributed remains inconclusive based on our immunocytochemistry results. The precise localization of the P2X<sub>4</sub> receptors in macula epithelial cells should be determined in the future using patch clamp techniques for different cell types or immunostaining using appropriate antibodies. Indeed, purinergic receptor expression on utricular supporting cells was suggested in two functional

studies;<sup>14,15</sup> however, these studies focused on the role of intracellular otopettrin 1 in regulating  $\text{Ca}^{2+}$  transport through  $\text{P}_2\text{X}$  and  $\text{P}_2\text{Y}$  receptors for otoconia formation and did not further evaluate the roles of specific purinergic receptor subunits. These supporting cells likely expressed  $\text{P}2\text{X}_2$  or both  $\text{P}2\text{X}_2$  and  $\text{P}2\text{X}_4$  based on the results of our study.

The electrophysiological and pharmacological findings in the present study identified non-selective cation absorption via  $\text{P}2\text{X}_2$  and  $\text{P}2\text{X}_4$  receptors in utricular TCs and macula. The evidence for the involvement of these receptors can be summarized as follows: First, the cation absorption current was induced only by ATP, but not by ADP, UTP, and UDP. Second, the ATP-induced cation absorption current was fully inhibited by Gd. Third, the  $\text{EC}_{50}$  values for the ATP derivatives were close to those of the  $\text{P}2\text{X}_2$  and  $\text{P}2\text{X}_4$  receptors. In fact, the  $\text{EC}_{50}$  values were closer to the  $\text{P}2\text{X}_2$  receptor, but the presence of  $\text{P}2\text{X}_4$  receptors could not be completely excluded if  $\text{P}2\text{X}_4$  receptors co-existed with  $\text{P}2\text{X}_2$  receptors, because the responses mediated by both receptors could be mixed. Therefore, we attempted to use different  $\text{P}2\text{X}$  receptor inhibitors (100  $\mu\text{M}$  suramin and 10  $\mu\text{M}$  PPADS for  $\text{P}2\text{X}_2$ , and 5  $\mu\text{M}$  5-BDBD for  $\text{P}2\text{X}_4$ ), and the pharmacological data obtained using these reagents revealed the involvement of both  $\text{P}2\text{X}_2$  and  $\text{P}2\text{X}_4$  receptors in ATP-induced cation absorption. Although most findings indicated the involvement of  $\text{P}2\text{X}_2$  and  $\text{P}2\text{X}_4$  receptors in cation transport in these areas, the existence of  $\text{P}2\text{Y}$  receptors in supporting cells and/or HCs cannot be completely excluded because minimal current changes

with a gentle slope, which can be observed in P2Y receptor-mediated cation absorption induced by ADP, UTP, and UDP, were identified in some cases in the HC area (Figure 4B., n=2). However, the current was not always observed in our experiments, and the current changes were tiny; therefore, the contribution of P2Y receptors to ATP-induced cation absorption is likely minimal.

The P2X<sub>2</sub> and P2X<sub>4</sub> receptors present in TCs and supporting cells likely provide a cation shunt for the regulation of inward current in HCs by ATP stimulation under conditions of excessive linear acceleration, although the localization of P2X<sub>4</sub> receptors in supporting cells remains inconclusive. This mechanism may both protect HCs and regulate HC sensitivity, which is very important in the maintenance of the vestibular system, especially in situations featuring excessive, abrupt acceleration stimuli, which can occur during driving, whiplash injuries during traffic accidents, aviation, space flight, and so forth. If this fine regulation by purinergic receptors is disrupted, vestibular HCs can be damaged, which ultimately leads to dizziness and balance disorders. Indeed, targeted disruption of the P2X<sub>2</sub> receptor gene in mice caused progressive hearing loss and increased susceptibility to noise stimulation without recovery.<sup>16,17</sup> Furthermore, P2X<sub>2</sub> receptor gene mutations in human are also reported to cause genetic progressive sensorineural hearing loss with an autosomal dominant inheritance pattern.<sup>17</sup> This observation implies that the P2X<sub>2</sub> receptor plays an important role in cochlear HC protection. Similarly, disruption of the P2X<sub>2</sub> and/or P2X<sub>4</sub> receptor gene may cause progressive or

mechanical stress (acceleration stimulus)-induced vestibular dysfunction by causing loss of their protective mechanisms, because those receptors are distributed in vestibular TCs and the macula, which are adjacent to sensory HCs. However, there is no study investigating vestibular function in the mouse model and patients with the P2X<sub>2</sub> receptor gene mutation. The future study about vestibular function in the animal model and patients will provide a clue in identifying the role of P2X<sub>2</sub> and P2X<sub>4</sub> receptors in vestibular function maintenance.

P2X<sub>4</sub> receptors may also be distributed in utricular HCs. Although several reports have demonstrated ATP-induced inward current and the presence of purinergic receptors in cochlear inner and outer HCs in different kinds of animals (P2X<sub>2</sub>, P2X<sub>3</sub>, and P2X<sub>7</sub> in inner HCs and P2X<sub>1</sub>, P2X<sub>2</sub>, P2X<sub>4</sub>, P2Y<sub>1</sub>, P2Y<sub>2</sub>, and P2Y<sub>4</sub> in outer HCs),<sup>4,12,18</sup> no studies have evaluated vestibular HCs. In cochlear HCs, purinergic receptors modulate sound transduction and neurotransmission by regulating inward currents and intracellular Ca<sup>2+</sup> concentrations.<sup>4</sup> Additionally, purinergic receptors are reportedly involved in regulating outer HCs motility, which is important in the amplification of basal membrane movement.<sup>12,18</sup> Because ATP is expected to be secreted in the vestibular system in response to acceleration stimulation, the purinergic receptor-mediated inward current in utricular HCs likely functions to modulate their sensitivity according to the severity of the linear acceleration stimulus.

Consequently, our study revealed that P2X<sub>2</sub> and P2X<sub>4</sub> receptor-mediated

cation absorption in utricular TCs and macula may serve as a protective or modulatory mechanism for the vestibular system. Although the phenomenon and role of purinergic signaling-induced cation transport in the vestibular system have yet to garner as much interest as those in the cochlea, they nevertheless likely play an important role in the maintenance of balance, as they do in the cochlea. Future further studies of P2X<sub>2</sub> and P2X<sub>4</sub> receptors in the vestibular system using genetically engineered mice and human patients with mutations will provide insight into the exact roles of purinergic receptors in the vestibular system for maintaining balance.

## V. CONCLUSION

P2X<sub>2</sub> and P2X<sub>4</sub> receptors regulate ion transport in the utricular transitional cells and macula by ATP stimulation in excessive linear acceleration situations. The P2X<sub>2</sub> and P2X<sub>4</sub>-mediated cation transport is likely to be involved in the protection of hair cell and modulation of signal transduction in hair cell during the event of excessive linear acceleration.

## REFERENCES

1. Moser T, Brandt A, Lysakowski A. Hair cell ribbon synapses. *Cell Tissue Res* 2006;326:347-59.
2. Lang F, Vallon V, Knipper M, Wangemann P. Functional significance of channels and transporters expressed in the inner ear and kidney. *Am J Physiol Cell Physiol* 2007;293:C1187-208.
3. Lee JH, Marcus DC. Purinergic signaling in the inner ear. *Hear Res* 2008;235:1-7.
4. Ito K, Dulon D. Purinergic signaling in cochleovestibular hair cells and afferent neurons. *Purinergic Signal* 2010;6:201-9.
5. Lee JH, Chiba T, Marcus DC. P2X2 receptor mediates stimulation of parasensory cation absorption by cochlear outer sulcus cells and vestibular transitional cells. *J Neurosci* 2001;21:9168-74.
6. Kim SH, Marcus DC. Endolymphatic sodium homeostasis by extramacular epithelium of the saccule. *J Neurosci* 2009;29:15851-8.
7. Jaffe LF, Nuccitelli R. An ultrasensitive vibrating probe for measuring steady extracellular currents. *J Cell Biol* 1974;63:614-28.
8. Reid B, Nuccitelli R, Zhao M. Non-invasive measurement of bioelectric currents with a vibrating probe. *Nat Protoc* 2007;2:661-9.
9. Coddou C, Yan Z, Obsil T, Huidobro-Toro JP, Stojilkovic SS. Activation and regulation of purinergic P2X receptor channels. *Pharmacol Rev* 2011;63:641-83.

10. Munoz DJ, Thorne PR, Housley GD, Billett TE. Adenosine 5'-triphosphate (ATP) concentrations in the endolymph and perilymph of the guinea-pig cochlea. *Hear Res* 1995;90:119-25.
11. White PN, Thorne PR, Housley GD, Mockett B, Billett TE, Burnstock G. Quinacrine staining of marginal cells in the stria vascularis of the guinea-pig cochlea: a possible source of extracellular ATP? *Hear Res* 1995;90:97-105.
12. Zhao HB, Yu N, Fleming CR. Gap junctional hemichannel-mediated ATP release and hearing controls in the inner ear. *Proc Natl Acad Sci U S A* 2005;102:18724-9.
13. Wangemann P. Comparison of ion transport mechanisms between vestibular dark cells and strial marginal cells. *Hear Res* 1995;90:149-57.
14. Kim E, Hyrc KL, Speck J, Lundberg YW, Salles FT, Kachar B, et al. Regulation of cellular calcium in vestibular supporting cells by otopetrin 1. *J Neurophysiol* 2010;104:3439-50.
15. Kim E, Hyrc KL, Speck J, Salles FT, Lundberg YW, Goldberg MP, et al. Missense mutations in Otopetrin 1 affect subcellular localization and inhibition of purinergic signaling in vestibular supporting cells. *Mol Cell Neurosci* 2011;46:655-61.
16. Housley GD, Morton-Jones R, Vlajkovic SM, Telang RS, Paramanathasivam V, Tadros SF, et al. ATP-gated ion channels mediate adaptation to elevated sound levels. *Proc Natl Acad Sci U S A*



2013;110:7494-9.

17. Yan D, Zhu Y, Walsh T, Xie D, Yuan H, Sirmaci A, et al. Mutation of the ATP-gated P2X(2) receptor leads to progressive hearing loss and increased susceptibility to noise. *Proc Natl Acad Sci U S A* 2013;110:2228-33.
18. Szucs A, Szappanos H, Toth A, Farkas Z, Panyi G, Csernoch L, et al. Differential expression of purinergic receptor subtypes in the outer hair cells of the guinea pig. *Hear Res* 2004;196:2-7.

## ABSTRACT(IN KOREAN)

난형낭 전이세포와 평형반에서의 P2X<sub>2</sub>와 P2X<sub>4</sub> 수용체 매개  
양이온 흡수

<지도교수 김성헌>

연세대학교 대학원 의학과

정준희

adenosine 5'-triphosphate (ATP)는 내이 상피세포에서 퓨린 수용체를 통한 이온 수송을 조절함으로써 내이 기능을 조절한다. 이 연구에서 선형 가속도 자극이 감지되는 쥐의 난형낭 평형반과 주변 전이세포에서의 퓨린 수용체 매개 양이온 수송을 조사하였다. ATP, adenosine 5'-diphosphate (ADP), uridine 5'-triphosphate (UTP), uridine 5'-diphosphate (UDP) 중에서 ATP (100  $\mu$ M)만 전이세포와 평형반에서 양이온 흡수 전류를 유도하였다. 이 전류는 gadolinium (100  $\mu$ M)을 적용하였을 때 대부분 완전히 억제되었다. 양이온 흡수 전류에 대한 작용제 효능 순서는 전이세포와 평형반 모두에서 ATP > 3'-O-(4-benzoyl-benzoyl) adenosine 5'-triphosphate (BzATP) >>  $\alpha,\beta$ -methyleneadenosine 5'-triphosphate ( $\alpha\beta$ meATP)였고 ATP, BzATP,  $\alpha\beta$ meATP의 EC<sub>50</sub> (절반의 최고 효과를 나타내는 농도) 값은 전이세포에서 27.2  $\mu$ M, 43.9  $\mu$ M, 34.5  $\mu$ M였고 평형반에서 20.7  $\mu$ M, 63.4  $\mu$ M, 2014.1  $\mu$ M였다 ( $\alpha\beta$ meATP의 EC<sub>50</sub> 값은  $\alpha\beta$ meATP의 낮은 효능으로 확실히 확인되지 않았다). ATP 유도 전류는 두 부위에서 suramin (100  $\mu$ M), pyridoxal phosphate-6-azo(benzene-2,4-disulfonic acid) (PPADS) (10  $\mu$ M), 그리고 5-(3-bromophenyl)-1,3-dihydro-2H-benzofuro[3,2-e]-1,4-diazepin-2-one

(5-BDBD) (5  $\mu$ M)에 의해 부분적으로 차단되었고 PPADS + 5-BDBD에 의해 거의 완전히 차단되었다. 면역세포화학법에서 전이세포와 평형반의 지지세포에 P2X<sub>2</sub> 수용체가 분포한다는 것이 확인되었다. 그러나 P2X<sub>4</sub> 수용체는 면역세포화학법으로 평형반에서 발견되지 않았지만 그것의 messenger ribonucleic acid (mRNA) 발현이 확인되었다. 이 결과들은 ATP가 난형낭 전이세포와 평형반에서 P2X<sub>2</sub>와 P2X<sub>4</sub> 수용체를 통해서 이온 흡수를 유도한다는 것을 나타낸다. P2X<sub>2</sub>와 P2X<sub>4</sub> 매개 양이온 수송은 과도한 선형 가속도 조건에서 양이온 이동으로 유모세포의 양이온 부담을 줄여서 유모세포를 보호할 것으로 생각된다.

---

핵심되는 말 : 난형낭, 전이세포, 평형반, 수용체, 양이온